

LEVEL

III
0026400

12
yw

A Further Study of the Space and Time Stability of a Narrowband Acoustic Signal in the Ocean: Short Range Results

**A Paper Presented at the 102nd Meeting of the
Acoustical Society of America, 1 December 1981,
Miami Beach, Florida**

**P. D. Koenigs
P. D. Herstein
D. G. Browning
Surface Ship Sonar Department**

**DTIC
ELECTE
JAN 18 1982
S D E**



**Naval Underwater Systems Center
Newport, Rhode Island / New London, Connecticut**

405918

AD A109668

DTIC FILE COPY

Preface

This document was prepared under the Ocean Measurements and Array Technology (OMAT) Program portion of the SEAGUARD Project sponsored by the Defense Advanced Research Projects Agency (ARPA Order No. 2976), Program Manager, V. Simmons, Tactical Technology Office; NUSC Project No. B69605, Program Manager, R. F. LaPlante.

Reviewed and Approved: 21 December 1981

A handwritten signature in black ink, appearing to read "Derek Walters", is centered on the page.

**Derek Walters
Surface Ship Sonar Department**

The authors of this document are located at the
New London Laboratory, Naval Underwater Systems Center,
New London, Connecticut 06320.

| REPORT DOCUMENTATION PAGE | | READ INSTRUCTIONS BEFORE COMPLETING FORM |
|---|--------------------------------------|---|
| 1. REPORT NUMBER TD 6605 | 2. GOVT ACCESSION NO. AD-A109 668 | 3. RECIPIENT'S CATALOG NUMBER |
| 4. TITLE (and Subtitle) A FURTHER STUDY OF THE SPACE AND TIME STABILITY OF A NARROWBAND ACOUSTIC SIGNAL IN THE OCEAN: SHORT RANGE RESULTS, A PAPER PRESENTED AT THE 102nd MEETING OF ASA, 1 DEC 1981, MIAMI BEACH, FLORIDA | | 5. TYPE OF REPORT & PERIOD COVERED |
| 7. AUTHOR(s) P. D. Koenigs, P. D. Herstein, and D. G. Browning | | 6. PERFORMING ORG. REPORT NUMBER |
| 9. PERFORMING ORGANIZATION NAME AND ADDRESS Naval Underwater Systems Center New London Laboratory New London, CT 06320 | | 8. CONTRACT OR GRANT NUMBER(s) |
| 11. CONTROLLING OFFICE NAME AND ADDRESS Defense Advanced Research Projects Agency Arlington, VA 22209 | | 10. PROGRAM ELEMENT, PROJECT, TASK AREA & WORK UNIT NUMBERS B69605 |
| 14. MONITORING AGENCY NAME & ADDRESS (if different from Controlling Office) <i>15) ✓ ARPA Order - 2976</i> | | 12. REPORT DATE 21 December 1981 |
| | | 13. NUMBER OF PAGES 14 |
| | | 15. SECURITY CLASS. (of this report) UNCLASSIFIED |
| | | 15a. DECLASSIFICATION / DOWNGRADING SCHEDULE |
| 16. DISTRIBUTION STATEMENT (of this Report) Approved for public release; distribution unlimited. | | |
| 17. DISTRIBUTION STATEMENT (of the abstract entered in Block 20, if different from Report) | | |
| 18. SUPPLEMENTARY NOTES | | |
| 19. KEY WORDS (Continue on reverse side if necessary and identify by block number) Bandwidth stability Signal stability Doppler shift Transmission phenomena Multipath phenomena Narrowband processes | | |
| 20. ABSTRACT (Continue on reverse side if necessary and identify by block number) This document presents the oral and visual presentation entitled "A Further Study of the Space and Time Stability of a Narrowband Acoustic Signal in the Ocean: Short Range Results," presented at the 102nd Meeting of the Acoustical Society of America, 1 December 1981, in Miami Beach, Florida. In the last of a three paper series on the space and time stability of a narrowband acoustic signal, results from short (16-17 nmi) ranges are | | |

20. (Continued)

presented. In contrast to the data obtained at longer ranges (P. D. Herstein, et al., J. Acoust. Soc. Am. 69 (S1), S33(A), 1981), an increased frequency spread was found in the received signal due to the greater number of possible raypaths at short ranges. A marked change in the character of the received signal was observed at ranges less than 70 nmi. Space and time variability are given for percentage Doppler shift and bandwidth. Comparison is made to data reported in the two previous papers and with predictions of the Multipath Expansion Option of the Generic Sonar Model.



**A Further Study of the
Space and Time Stability of a
Narrowband Acoustic Signal in the Ocean:
Short Range Results**

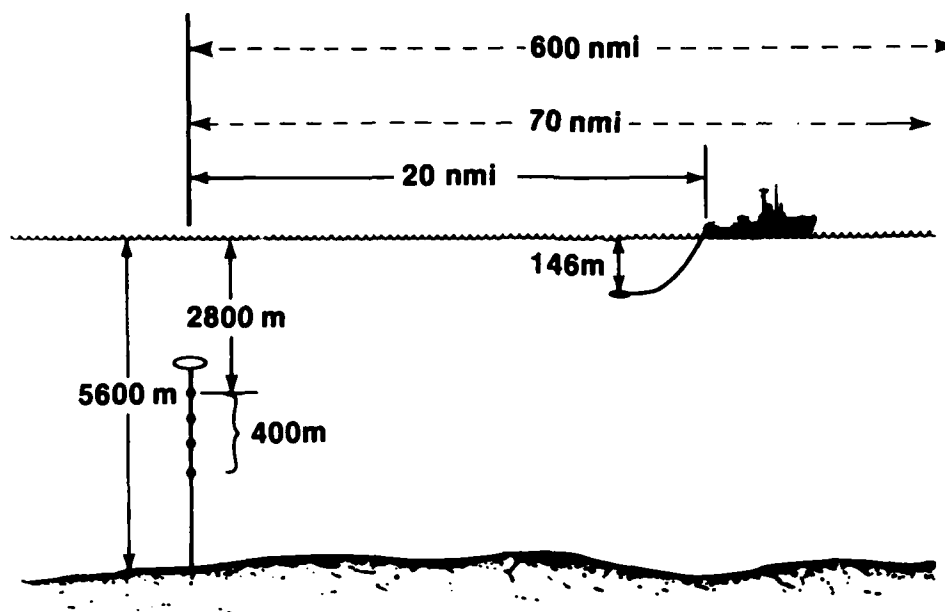
Introduction

Our initial interest in characterizing the transmission of low frequency narrowband signals was to determine if the spatial inhomogeneity and temporal instability of the ocean caused narrowband shipping generated noise to be transformed into broadband noise.

— First viewgraph, please. —

| | |
|--------------------|-------------------------------------|
| Accession For | |
| NTIS GRA&I | <input checked="" type="checkbox"/> |
| DTIC TAB | <input type="checkbox"/> |
| Unannounced | <input type="checkbox"/> |
| Justification | |
| By _____ | |
| Distribution/ | |
| Availability Codes | |
| Dist | Avail and/or Special |
| A | |





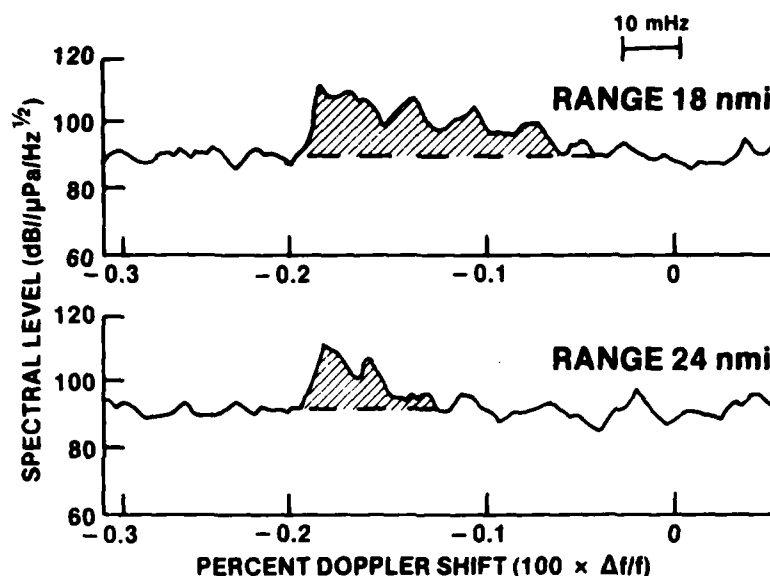
Viewgraph 1

At the last two meetings of the society, we addressed the space and time variability of narrowband signals in the ocean at ranges of 70 and 590 nautical miles. Today we will present the results of our analyses conducted with data obtained at closer ranges and then look at the overall range dependence of our results.

Our experimental data were obtained using the configuration shown here. The ship towed a very stable low frequency continuous wave source at a constant depth and speed in the North American Basin. The signals were received on four hydrophones vertically spanning 400 meters centered near the middle of the water column. The range intervals we selected for our analysis were centered near 20, 70, and 590 nautical miles. Now, let's take a look at the data obtained at the 20 nautical mile range interval.

— Next viewgraph, please. —

REPRESENTATIVE RECEIVED SIGNAL SPECTRA AVG TIME 710 sec



Viewgraph 2

Shown here are two representative power spectra of the signals received on one of the hydrophones. The X-axis is percent Doppler shift and is negative because we are opening range. In the upper spectrum, the source-receiver separation is about 18 nautical miles. Note that there is considerable frequency spread and the shape of the spread somewhat resembles a sawtooth. In the lower figure, the source-receiver separation is about 24 nautical miles. A quick comparison of the spectra indicates the signal bandwidth in the lower figure is considerably narrower than in the upper figure. Thus, one could infer that signal bandwidth is *decreasing* with *increasing* range. (This will be substantiated further in viewgraphs 8 and 9.)

— Next viewgraph, please. —

DATA MATRIX

| | T_1 | T_2 | ■ | ■ | ■ | T_N | TIME AVERAGES |
|-------------------|-----------------|-----------------|---|---|---|-------------|-----------------|
| H_1 | ● | ● | ● | ● | ● | ● | \bar{T}_{H_1} |
| H_2 | ● | ● | ● | ● | ● | ● | \bar{T}_{H_2} |
| H_3 | ● | ● | ● | ● | ● | ● | \bar{T}_{H_3} |
| H_4 | ● | ● | ● | ● | ● | ● | \bar{T}_{H_4} |
| SPACE AVERAGES | \bar{S}_{T_1} | \bar{S}_{T_2} | | | | \bar{S}_N | |

Viewgraph 3

The results of our analysis, which yield classical 3 dB bandwidths by using second-order polynomial fits to spectra, are presented in this way. The 4 hydrophones are designated H_1 through H_4 . The overlapped and windowed data from each hydrophone were processed in 12 minute-intervals yielding an effective Discrete Fourier Transform filter bandwidth of 2 millihertz. Therefore, for a two-hour data set near 20 nautical miles, we obtained 13 space averages by averaging over the 400 meter vertical extent and 4 time averages by averaging the data from a single hydrophone over the 13 available time intervals. This makes it possible to compare bandwidth changes as functions of space and time.

— Next viewgraph, please. —

BANDWIDTH STATISTICS

NEAR RANGE RESULTS (16-27 nmi)

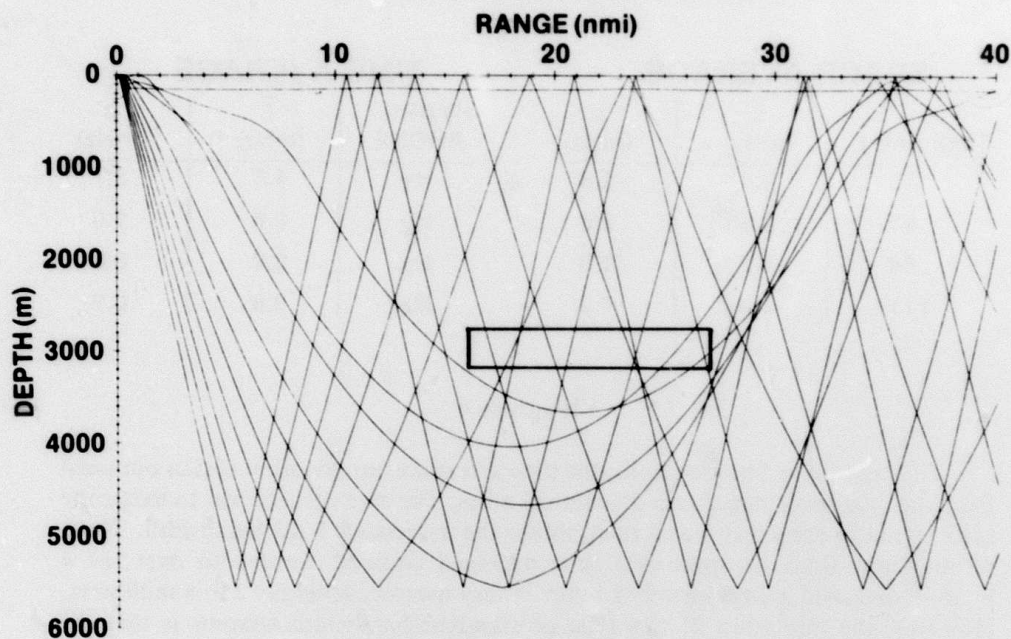
| SPACE AVERAGE | | | TIME AVERAGE | | |
|---------------|--------------------|-------------------|-----------------|--------------------|-------------------|
| TIME (min) | \bar{S} (mHz) | σ (mHz) | HYDRO- PHONE | \bar{T} (mHz) | σ (mHz) |
| 18 | 3.4 | 0.6 | H ₁ | 4.5 | 2.7 |
| 45 | 5.3 | 2.8 | H ₂ | 3.8 | 1.0 |
| 84 | 4.2 | 0.8 | H ₃ | 3.8 | 0.8 |
| 111 | 3.0 | 0.3 | H ₄ | 3.9 | 0.9 |

Viewgraph 4

The table shown here contains the time and space bandwidth statistics obtained from the data set centered near 20 nautical miles. The method used was to locate the peak signal in the spectra and then obtain the associated 3 dB bandwidth. These results show that the space and time averaged classical bandwidth over the 4 hydrophones and approximately 2 hours is very narrow, generally 3 to 6 millihertz. However, the limitation of this type of standard bandwidth analysis is that the measurement does not include other lower spectral peaks if they are present and frequency resolvable.

— Next viewgraph, please. —

RAY DIAGRAM
146 M SOURCE DEPTH
INCLINATION ANGLES FROM
-30 TO 0 DEG IN 3 DEG STEPS

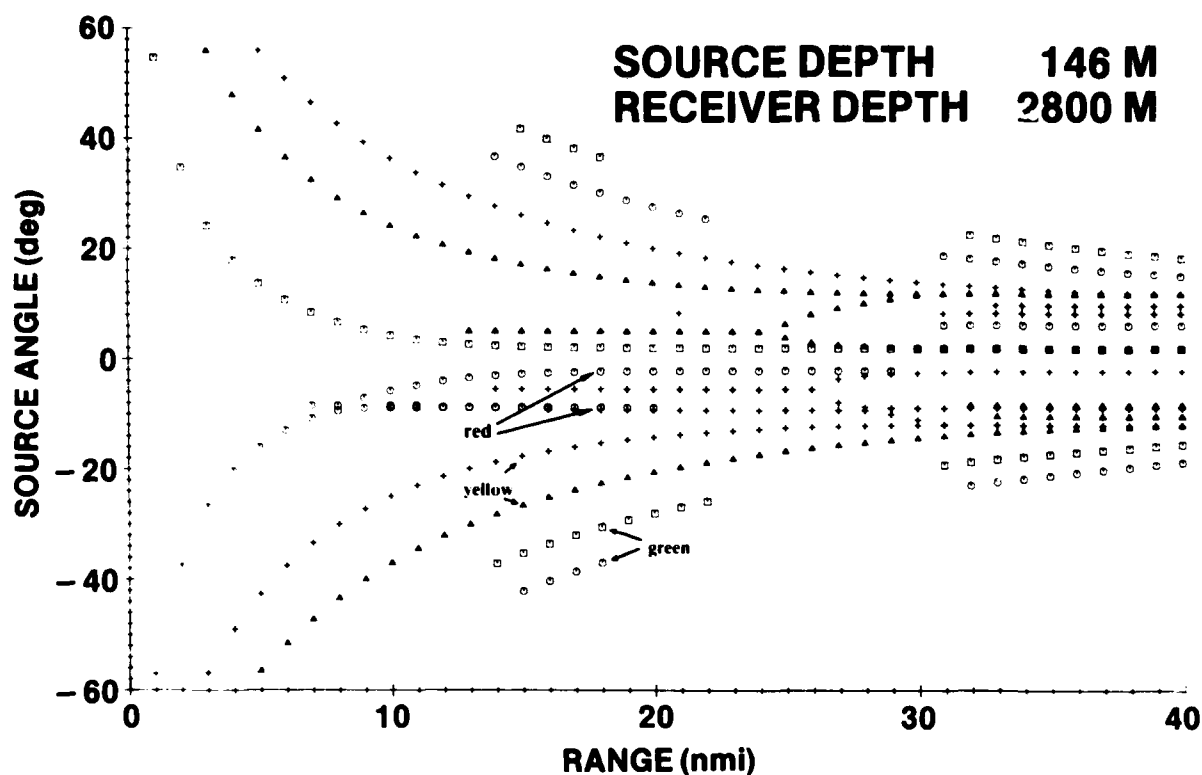


Viewgraph 5

We have already shown that our spectral data do contain several frequency resolvable peaks that exhibit significant range dependence. The reasons for this frequency spread can be related to a moving acoustic source and a multipath environment. To obtain an estimate of the possible multipaths that might be present, we used the predictions of the multipath expansion option of the generic sonar model developed by Weinberg. This ray plot shows the region that was covered by this data set. Since the source is opening range, we are sweeping our 400 meter aperture across the rays as shown by the window near the center of the figure.

— Next viewgraph, please. —

SOURCE ANGLE VS RANGE

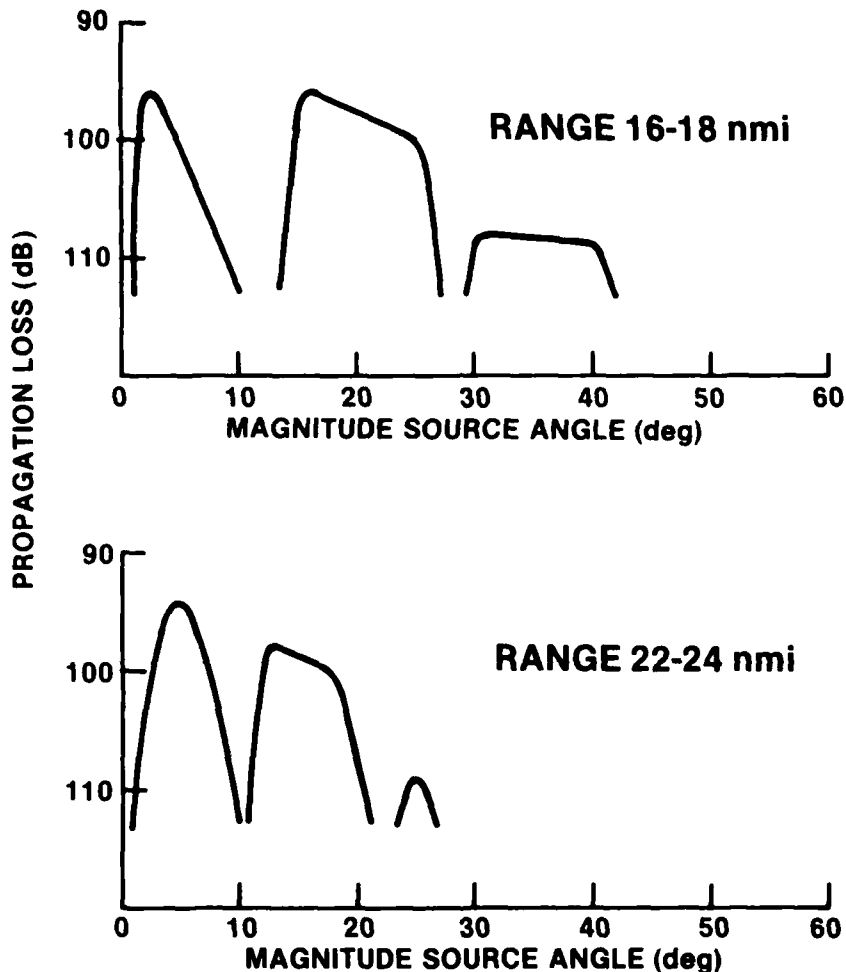


Viewgraph 6

The modeling program identifies principal source or launch angles of eigenrays that eventually intercept the receiver. Shown here are source angles as a function of range for a source at 146 meters and a receiver at 2800 meters. The eigenrays highlighted by green, near minus 40 degrees, are bottom bounce rays that have undergone two bottom interactions. Those rays highlighted by yellow have undergone a single bottom interaction. Those identified by red have not interacted with the bottom. A similar identification can be made for all the other eigenrays. Note at these ranges the strong dependence of source angle with range. What is not illustrated here are relative intensities. So let's take a look at modeled intensity versus source angle for the two ranges indicated by the dashed lines on this figure.

— Next viewgraph, please. —

MODELED PROPAGATION LOSS VS MAGNITUDE OF SOURCE ANGLE



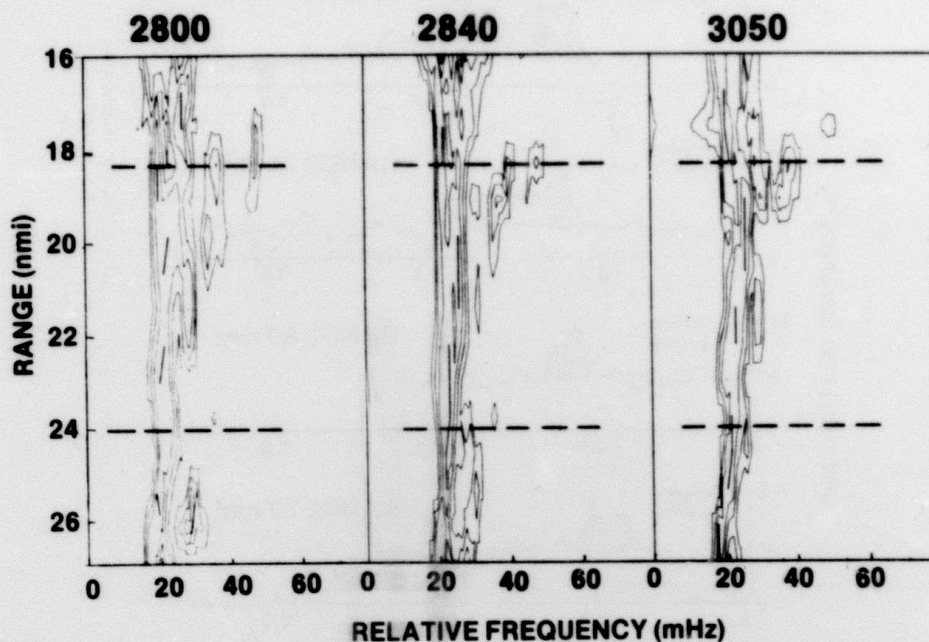
Viewgraph 7

Shown in the upper figure is the modeled propagation loss as a function of the absolute value of the source angle near 18 nautical miles. The principal reason for the different levels at this range is the number and incident angles of the bottom interactions the signals undergo before reaching the receiver. The lower figure represents the modeled results obtained near 24 nautical miles. At this range the only eigenrays we expect to resolve are those that either interact with the bottom once or not at all. From basic physics we know that the Doppler shift for moving sources and stationary receivers is dependent on radial speed. Our source is moving at a nearly constant velocity near the ocean surface so we expect a Doppler shift that is dependent on the magnitude of the source angle. This results in frequency resolvable spectral peaks being generated from a CW source.

— Next viewgraph, please. —

SIGNAL BANDWIDTH VS RANGE AT THREE DEPTHS

HYDROPHONE DEPTH (m)

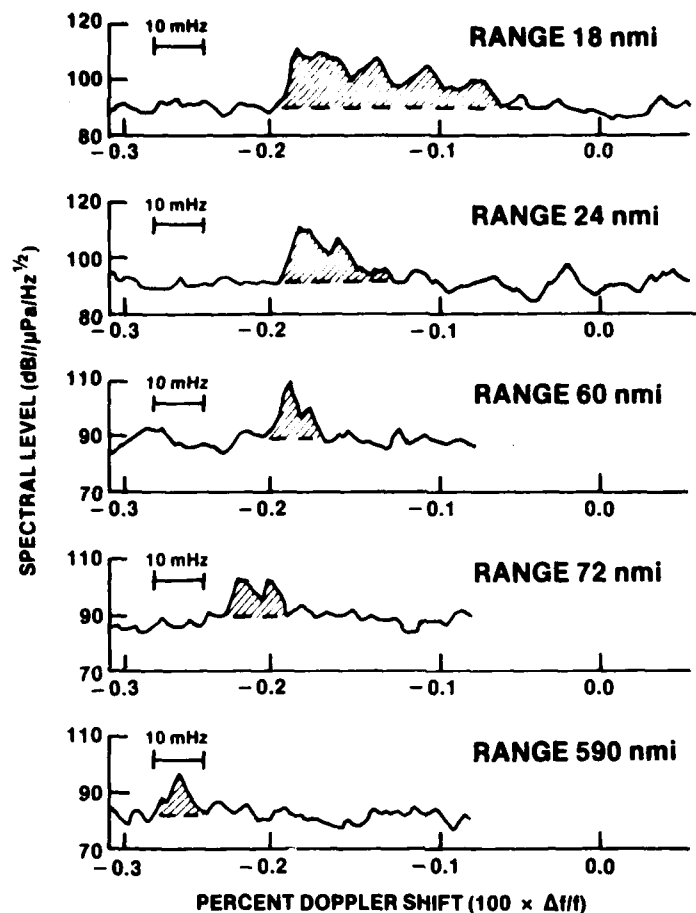


Viewgraph 8

This figure depicts the range dependence of measured signal bandwidth. Shown here are the 3, 6, and 9 dB bandwidth contours as a function of range for 3 hydrophones. The dashed lines mark the ranges at 18 and 24 nautical miles. With the receiver at 18 nautical miles, signals with relatively high source angles and hence low Doppler shift are being received. This results in substantial frequency smear and large bandwidths. However, at 24 nautical miles only those signals with small launch angles are of sufficient intensity to rise above the ocean noise. This results in a very narrow bandwidth. Also apparent, at least qualitatively, is a dependence of bandwidth on depth as one would expect in a rapidly changing multipath structure.

— Next viewgraph, please. —

REPRESENTATIVE RECEIVED SIGNAL SPECTRA **AVG TIME 710 sec**



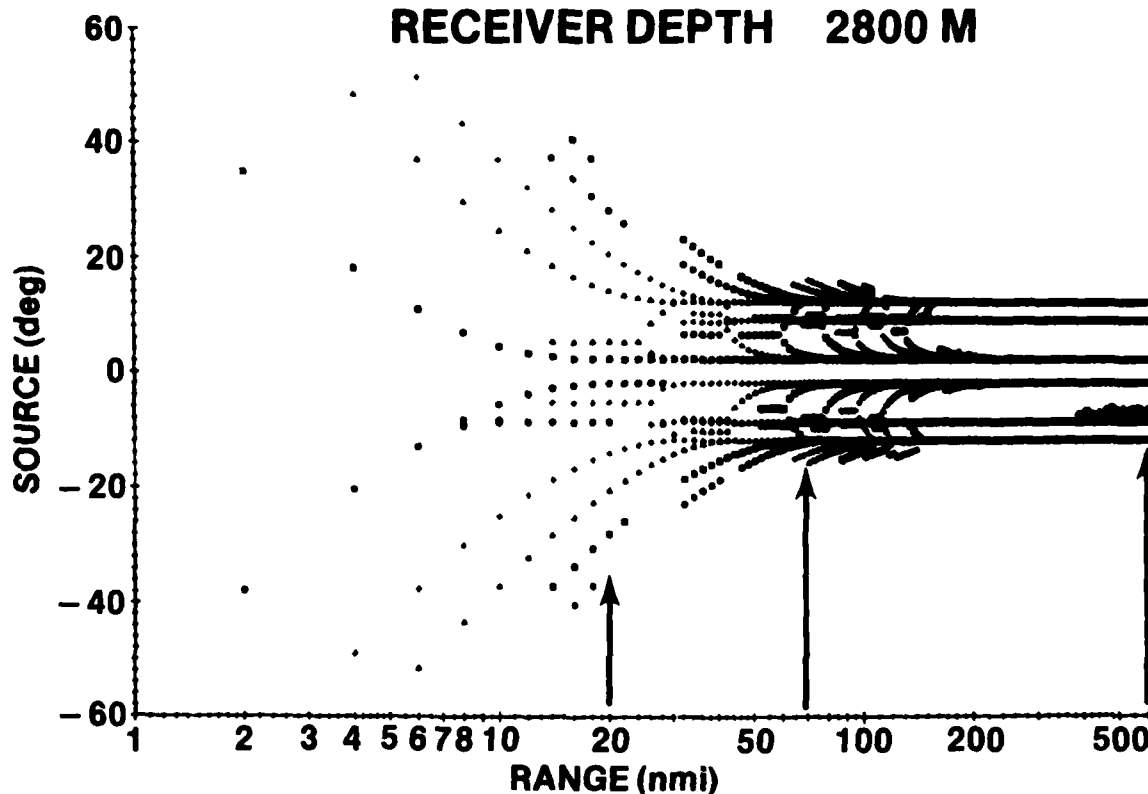
Viewgraph 9

Now that we have taken a detailed look at the signal bandwidths at ranges within a convergence zone we would like to present an overview of the range dependence of signal bandwidth for moving sources and a multipath environment. Shown here are five representative spectra obtained on a single hydrophone. The upper two spectra, obtained from within the first convergence zone, were just discussed and you can see there is a substantial bandwidth associated with the signal. The third and fourth spectra were obtained at intermediate ranges of 60 and 72 nautical miles. The bottom figure represents a typical spectra of the received signal at a separation distance of 590 nautical miles and depicts a very narrow bandwidth. There are two points we would like to make with this figure. First, it's relatively easy to generalize and state that the total signal bandwidth decreases as range increases. Secondly, it appears that principal eigenrays, when they are resolvable appear to have classically defined 3 dB bandwidths that are very narrow and independent of range. The shift in the observed minimum value of percent Doppler shift as a function of ranges is due to slightly different ship speeds. The fact that it appears to increase monotonically with range is purely coincidental.

— Next viewgraph, please. —

SOURCE ANGLE VS RANGE

SOURCE DEPTH 146 M
RECEIVER DEPTH 2800 M

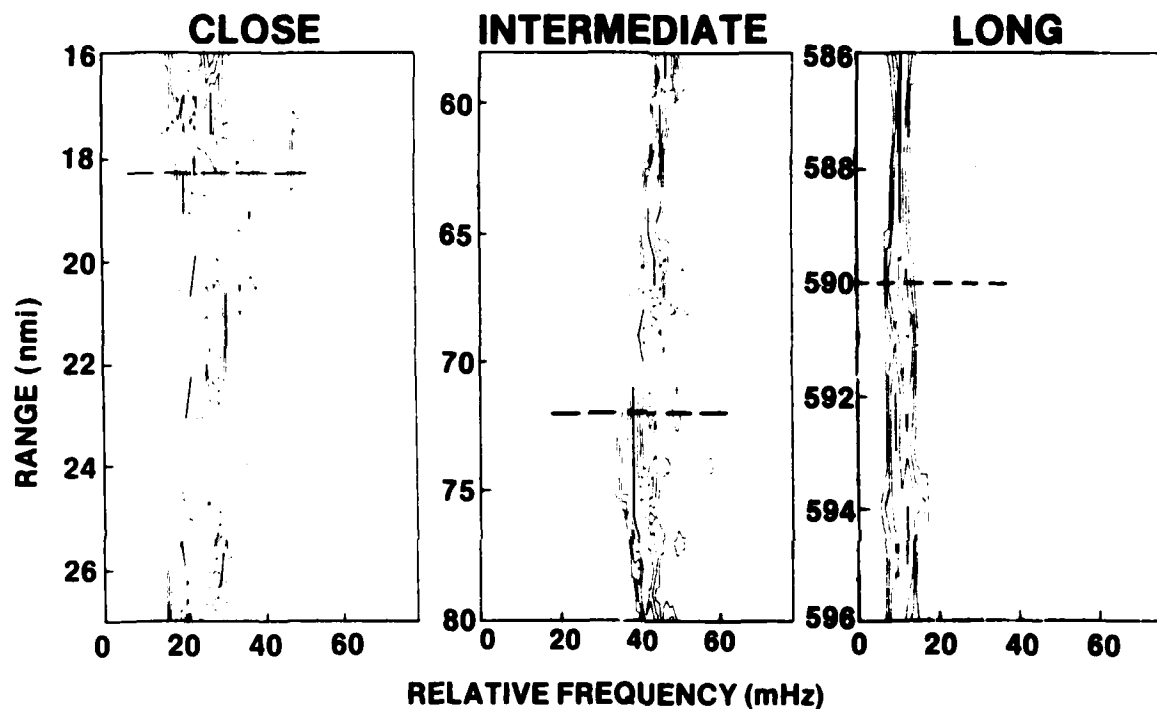


Viewgraph 10

Shown here are the model results of source angle versus range from 2 to 600 nautical miles for the dominant eigenrays. The arrows near the bottom scale on this figure indicate the three range intervals that we have investigated in detail. Since the frequency smear or bandwidth is related to the spread in launch angles for moving sources it is easy to see (for our experimental conditions) that substantial frequency smear can occur at relatively close ranges and the smear or bandwidth will in general decrease as range increases. Furthermore, if one is able to resolve the eigenrays, the frequency smear due to Doppler shifting is quite small.

— Next viewgraph, please. —

SIGNAL BANDWIDTH VS RANGE FOR THREE RANGE REGIMES (HYDROPHONE H₁)



Viewgraph 11

Shown here for comparative purposes are the detailed 3, 6, and 9 dB signal bandwidth contours obtained from one hydrophone at the three range intervals previously noted. The figure on the left is the closest range interval. It is quite easy to see that the signal received at 18 nautical miles has a total 6 dB bandwidth contour of nearly 40 millihertz, and, furthermore, the multipath structure is resolvable in the frequency domain. The dominant eigenrays in this case are resolvable and exhibit very narrow bandwidths on the order of 4 millihertz. At the intermediate ranges, shown here in the center figure, most of the eigenrays originating at large source angles with respect to the horizontal plane are attenuated through multiple bottom interactions so that only a few significant eigenrays are remaining. Thus, the signal bandwidth at this range is much narrower than at 18 nautical miles but still exhibits some spreading, particularly near 72 nautical miles. At long ranges, shown here on the right, there remains only the one dominant group of eigenrays with similar launch angles that have not interacted with the bottom; hence, the signal bandwidth is very narrow and (as illustrated here) has little range dependence.

— Next viewgraph, please. —

CONCLUSIONS

FOR A CONSTANT VELOCITY SOURCE:

1. TOTAL SIGNAL BANDWIDTH GENERALLY DECREASES AS RANGE INCREASES.
2. BANDWIDTH OF RESOLVABLE EIGENRAYS IS VERY NARROW AND INDEPENDENT OF RANGE.
3. MULTIPATH STRUCTURE AND BOTTOM REFLECTION COEFFICIENT ARE KEY FACTORS IN RANGE DEPENDENCE OF BANDWIDTH.

Viewgraph 12

We can summarize our results as follows. For an acoustic source moving with constant velocity, the received total signal bandwidth will in general decrease as range increases. However, the bandwidth of frequency resolvable eigenrays is very narrow (typically less than 4 millihertz) and nearly independent of range. These results can be directly related to the multipath structure, bottom reflection coefficient and Doppler effect.

— Viewgraph off, please. —

Thank you.

Initial Distribution List

| ADDRESSEE | NO. OF COPIES |
|--|---------------|
| ARPA Program Office | 1 |
| ARPA (R. Fossum, G. Sigman, W. Phillips, T. Kooij) | 4 |
| ARPA Research Center (E. Smith) | 1 |
| A3NRE&S (G. Cann) | 1 |
| CNM (MAT-08L, D. F. Parrish; MAT 0724, CAPT E. Young) | 2 |
| NAVELEX (PME-124, CDR D. Jones; CAPT. D. Murton, Code 612) | 2 |
| NAVSEASYSKOM (Code 63R, Dr. C. D. Smith; Code 63RA, Dr. R. W. Farwell) | 2 |
| NAVPGSCOL (Prof. C. N. K. Mooers; Professor H. Medwin) | 2 |
| NORDA (Code 110; Code 115, R. Martin; Code 340, S. Marshall; Code 500, L. Soloman; Code 521, C. Stuart; Library) | 6 |
| NOSC (Code 5313B, Dr. J. R. Lovett; Library) | 2 |
| NR (B. Adams, R. Heitmeyer, W. Moseley, R. Rojas, Dr. A. Berman, Dr. K. M. Guthrie, Dr. W. Carey, Dr. O. I. Diachok, Dr. R. L. Dicus) | 9 |
| NUSC Tudor Hill Laboratory (Library) | 1 |
| Office of Naval Research (Code 480, Dr. G. R. Hamilton; Code 421, Dr. L. E. Hargrove) | 2 |
| SSPO (P. Selwyn) | 1 |
| SACLANT ASW RESEARCH CENTRE (R. Goodman, R. Wagstaff) | 2 |
| NADC (Library) | 1 |
| NCSC (Library) | 1 |
| NSWC (Library) | 1 |
| CEL (Library) | 1 |
| DWTNSRDC (Library) | 1 |
| U. S. Naval Oceanography Command Center (CDR R. R. Miller) | 1 |
| ORI (R. Doolittle, E. Moses, V. Simmons) | 3 |
| Raytheon Submarine Signal Division (R. Dluhy, R. Pridham, C. Kaufman) | 3 |
| MAR, Inc. (H. Bakewell, C. Veitch) | 2 |
| BBN (J. Heine, G. Shepard, P. W. Smith, Jr., H. Cox) | 4 |
| Admiralty Underwater Weapons Establishment (D. Stansfield; Dr. D. E. Weston) | 2 |
| University of New Hampshire (A. S. Westneat) | 1 |
| Computing Devices Co. (K. N. Braun) | 1 |
| Marine Physical Laboratory, SCRIPPS (B. Williams, F. H. Fischer) | 2 |
| Institute of Geophysics, SCRIPPS (Dr. W. H. Munk) | 1 |
| RPI Math Sciences Dept (W. Siegmann) | 1 |
| University of Houston (Dr. B. D. Cook) | 1 |
| Royal Australian Navy Research Laboratory (Dr. M. Lawrence) | 1 |
| Instituto de Pesquisas da Marinha (CDR C. Parente) | 1 |
| Yale University (Dr. J. G. Zornig) | 1 |
| Case Western Reserve University (Dr. E. B. Yeager) | 1 |
| Georgetown University (Dr. W. G. Mayer) | 1 |
| University of Tennessee (Dr. M. A. Breazeale) | 1 |
| University of Rhode Island (Dr. F. Diete, Prof. J. Knauss, Dr. P. Stephanishen) | 3 |
| University of California, Santa Cruz (Dr. S. Flatte) | 1 |
| ARL, University of Texas (Dr. L. Hampton) | 1 |
| University of Bath (Dr. H. O. Berkday) | 1 |
| Defence Research Est. Atlantic (Dr. H. M. Merklinger) | 1 |
| Defence Research Est. Pacific (Dr. R. Chapman) | 1 |
| Technical University of Denmark (Dr. L. Bjorno) | 1 |
| Universite Louis Pasteur (Professor S. Candau) | 1 |
| Defence Research Centre (Dr. D. H. Brown) | 1 |
| SENID (Dr. J. Novarini) | 1 |
| DTIC | 12 |